

to the  $d_{z^2}$ -like which would diminish the denominators of the perturbation terms in eq 12 making major contributions to  $\delta g_{xx}$  and  $\delta g_{yy}$  which are of the type in Figure 1b and hence enhance the departures from free-electron character. However, with this explanation, to explain the significant observed asymmetry<sup>36</sup> in  $g_{xx}$  and  $g_{yy}$ , one would have to assume the  $d_{xz}$ -like level to be significantly higher than the  $d_{z^2}$ -like level. This could be the result of the asymmetric observed<sup>40</sup> disposition of the NO bond in horse-heart NOHb in contrast to the symmetrical situation<sup>34</sup> we have used. This possibility should be tested in the future, but it is also possible that there may be some asymmetry produced in the electron distribution due to the interaction between some groups on the protein chain and the heme unit, as pointed out for ferricyt *c*, section IIIa. This situation would be similar in nature to, but different in detail from, that found<sup>43</sup> for met Mb, where one needed an asymmetry between diagonally opposite pyrrole rings to explain asymmetries in single-crystal <sup>14</sup>N hyperfine data.<sup>44</sup>

To reinforce some of these conclusions, it will be worthwhile to carry out, as in the case of ferricyt *c*, perturbation calculations of the present type with wave functions and energy levels from more first-principle calculations, such as by the Hartree-Fock procedure<sup>27-29</sup> and the approximate MS-X $\alpha$  approach.<sup>30,31</sup> The influence of spin-orbit interaction on the energy-level spacings is not expected to be as important a contributing factor as in ferricyt *c*, where the important energy difference for  $g_{zz}$ ,  $g_{xz}$ , and  $g_{yz}$  was the small one between  $d_{xz}$  and  $d_{yz}$  which was very significantly influenced by spin-orbit interaction. In the present case it is the relatively large separation between the  $d_{z^2}$ -like and other levels that is involved, which is percentage-wise not as significantly

influenced by spin-orbit interaction. In this system also, it would be desirable to study the influence of other mechanisms discussed earlier for ferricyt *c*, particularly the exchange polarization mechanism. In this connection, one would also like to examine how well the <sup>14</sup>N hyperfine tensor for the NO group, after incorporation of exchange polarization, compares with experiment<sup>36-39</sup> both with respect to the magnitudes of the principal components and the orientations of the principal axes. In particular, it would be interesting to see if one of the principal components of the A tensor does, in fact, coincide with or lie close to the NO bond direction as has been assumed in earlier empirical analysis<sup>36</sup> for determination of the Fe-N-O bond angle.

#### IV. Conclusion

The investigations reported in the present work for two low-spin hemoglobin derivatives indicate that the perturbation approach for the **g** tensor with molecular orbital wave functions and energy levels provides reasonable overall agreement with experiment and can therefore be used as a check on the electronic charge and spin distributions over hemoglobin derivatives, which can complement their hyperfine properties in this respect. Since this procedure directly uses the wave functions and energy levels from electronic structure investigations and does not use any parametric fits to experimental data, the comparison of the results with experiment can be used to draw conclusions regarding improvements in the calculated electronic structure and other mechanisms contributing to the **g** tensor. Two such mechanisms are discussed and the role of one of them, the exchange polarization mechanism, is emphasized. It is hoped that similar investigations, as in the present work, of additional low-spin hemoglobin derivatives will be carried out in the future to test the general applicability of the conclusions obtained here.

Registry No. ferricyt *c*, 9007-43-6.

(43) Mishra, K. C.; Mishra, S. K.; Scholes, C. P.; Das, T. P. *J. Am. Chem. Soc.* **1983**, *105*, 7553-7556.

(44) Scholes, C. P.; Lapidot, A.; Mascarenhas, R.; Inubushi, T.; Isaacson, R. A.; Feher, G. *J. Am. Chem. Soc.* **1982**, *104*, 2724-2735.

## Structural Dependence of the Singlet-Triplet Energy Gap of the Tetramethylene Biradical

C. Doubleday,\*† J. McIver,\*‡ and M. Page§

Contribution from the Department of Chemistry, Columbia University, New York, New York 10027, the Department of Chemistry, State University of New York at Buffalo, Buffalo, New York 14214, and the Laboratory for Computational Physics, Naval Research Laboratory, Washington, D.C. 20375. Received May 8, 1985

**Abstract:** Ab initio calculations were performed on the tetramethylene biradical with use of a 2-configuration MCSCF wave function and the 3-21G basis set. The singlet-triplet energy gap  $E_{ST}$  was calculated as a function of the three internal rotation angles, both with planar  $sp^2$  terminal methylene groups and with pyramidal terminal methylenes. Over most of the surface through-bond coupling dominates  $E_{ST}$ , and for certain symmetric structures this effect is analyzed. With regard to the intersystem crossing process, the important result is the extraordinary ease with which singlet-triplet intersections are encountered during the lifetime of the triplet biradical.

Triplet 1,4-biradicals are now familiar reactive intermediates in organic chemistry.<sup>1</sup> Despite the familiarity, we have only a rudimentary understanding of their lifetimes and product distributions. This is not surprising in view of the complexity of the intersystem crossing (isc) problem. A major hindrance to investigators has been the absence of any firm knowledge of the relation between biradical structure and the singlet-triplet (S-T) energy gap.

A complete theoretical description of isc in 1,4-biradicals is currently intractable. Certainly, the least one requires is the location of important regions of the S-T intersection hypersurface, and the present calculations are directed toward that goal. While this still leaves us far from the ultimate goal of calculating the isc rate constant a priori, the location of the S-T intersection places

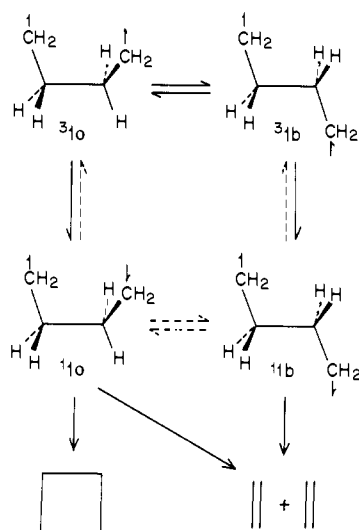
(1) (a) Wagner, P. J. *Acc. Chem. Res.* **1971**, *4*, 168. (b) Wagner, P. J. In "Rearrangements in Ground and Excited States"; deMayo, P., Ed.; Academic Press: New York, 1980; Vol. 3, pp 402-439. (c) Platz, M., Ed. *Tetrahedron* **1982**, *38* (6), 733-867. (d) Dervan, P. B.; Dougherty, D. A. In "Diradicals"; Borden, W. T., Ed.; Wiley: New York, 1981; pp 107-149. (e) Engel, P. S. *Chem. Rev.* **1980**, *80*, 99.

\*Columbia University.

†State University of New York at Buffalo.

§Naval Research Laboratory.

Scheme I



qualitative restrictions on the isc process.

Ab initio calculations were performed on the parent 1,4-biradical tetramethylene, **1**, whose triplet state can exist in either the gauche (**1a**) or anti (**1b**) forms shown in Scheme I. This kinetic scheme summarizes our model for the dynamics of triplet-derived tetramethylene derivatives. It was employed by Bartlett and Porter<sup>2a</sup> and has been used, with variation and modification, by a number of authors.<sup>2b-7</sup> There are three features of the model. (1) Thermal equilibration on the triplet potential energy surface (PES) is faster than isc. This is reasonable in view of the low barriers for gauche-anti interconversion<sup>8</sup> and the triplet lifetime of ca. 100 ns<sup>5-7</sup> for typical tetramethylene derivatives. (2) Isc is much slower than subsequent product formation on the singlet PES. That is, the lifetime of a triplet-derived biradical is governed by isc rather than product formation. A considerable body of evidence supports this.<sup>2-7</sup> (3) Product formation on the singlet PES is faster than gauche-anti interconversion. This is also strongly supported by experimental evidence.<sup>2,3,5,6</sup> The dotted lines in Scheme I indicate the kinetically unimportant interconversion. In view of our recent hypothesis that **1a** behaves like an entropically bound intermediate,<sup>9</sup> we do not necessarily imply that **1b** is also an intermediate, only that interconversion between the **1a** and **1b** geometries is slower than product formation.

A number of experiments have demonstrated that the cyclization/fragmentation product ratio depends on whether the 1,4-biradical is generated in the singlet or triplet state.<sup>2,10</sup> Usually a greater amount of fragmentation is observed in the triplet reaction, but sometimes the reverse is true.<sup>2,10</sup> No obvious pattern has yet emerged, and the cyclization/fragmentation ratio typically changes by less than half an order of magnitude. Various ra-

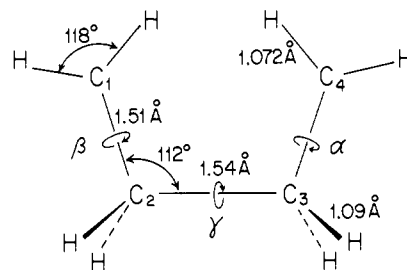


**Figure 1.** Internal coordinates for **1** with a planar,  $sp^2$  arrangement of the terminal methylenes, used in calculating Figures 2-7. The  $C_{2v}$  geometry shown here is the (0,0,0) reference for the dihedral angles  $\alpha, \beta, \gamma$ .  $\gamma$  is defined by fixing  $C_2, C_3, C_4$  and rotating  $C_1$ .

tionalizations of this effect are possible. If in fact all products are formed directly from a 1,4-biradical, Scheme I offers a unifying framework within which to interpret all known results.  $k_{isc}$  is expected to depend on the biradical structure, and this dependence is carried over to the product ratio as a result of feature 3 of the working model.

According to Scheme I, a triplet-derived biradical first equilibrates among its conformers, then undergoes isc to the singlet, then forms products directly from the singlet conformer produced by isc. To predict the product ratio we need to know three things: the equilibrium constant for  $^3\mathbf{1a} \rightleftharpoons ^3\mathbf{1b}$ , the relative isc rate constants in **1a** and **1b**, and the relative rates of product formation on the singlet PES. We have made progress toward answering the last question by showing that the barrier to cyclization is largely entropic.<sup>9,11</sup> Much additional work is needed to predict the singlet-derived product ratios. The triplet equilibrium constant can be calculated in a straightforward way by a conventional quantum chemical calculation of the local minima on the triplet PES.<sup>12</sup> Our interest here is in the more difficult question of isc rates.

The study of reactions involving surface crossings is much more complex than single-PES chemistry. One problem is that the intersection of two  $N$ -dimensional surfaces is itself a surface of  $N - 1$  dimensions, the locus of which is not obvious a priori. The most serious problem is that there is no generally applicable, tractable method for obtaining the crossing rate, even if both surfaces are known. This contrasts with the situation in single-PES chemistry, where one has transition-state theory<sup>13a</sup> and RRKM<sup>13b</sup> theory. There, a major role is played by stationary points on the PES (minima and saddle points). In surface-crossing problems saddle points play no direct role, and minima affect the crossing rate mainly by determining the number of molecules available for crossing at a given energy (the Boltzmann factor). *The main focus of one's attention thus shifts from locating and characterizing stationary points to locating the energetically accessible intersections between the two surfaces.* We have therefore concentrated on the S-T energy gap as a function of the loose modes: the three internal rotations and the pyramidalization of the terminal methylenes.

## Method

We used the split-valence 3-21G basis set<sup>14a</sup> with the 2-configuration MCSCF (2CSCF) wave function,<sup>15</sup> equivalent in this

(2) (a) Bartlett, P. D.; Porter, N. *J. Am. Chem. Soc.* **1968**, *90*, 5317. (b) Schultz, P.; Dervan, P. *J. Am. Chem. Soc.* **1982**, *104*, 6660.

(3) (a) Doubleday, C. *Chem. Phys. Lett.* **1979**, *64*, 67. (b) Doubleday, C. *Chem. Phys. Lett.* **1981**, *77*, 131. (c) Doubleday, C. *Chem. Phys. Lett.* **1981**, *79*, 375. (d) Doubleday, C. *Chem. Phys. Lett.* **1981**, *81*, 164. (e) Doubleday, C. *Chem. Phys. Lett.* **1982**, *85*, 65.

(4) DeKanter, F.; Kaptein, R. *J. Am. Chem. Soc.* **1982**, *104*, 4759.

(5) (a) Caldwell, R. A.; Majima, T.; Pac, C. *J. Am. Chem. Soc.* **1982**, *104*, 629. (b) Caldwell, R. A.; Creed, D. *J. Phys. Chem.* **1978**, *82*, 2644. (c) Caldwell, R. A.; Sakuragi, H.; Majima, T. *J. Am. Chem. Soc.* **1984**, *106*, 2471.

(6) (a) Scaiano, J. C. *Acc. Chem. Res.* **1982**, *15*, 252. (b) Scaiano, J. C. *Tetrahedron* **1982**, *38*, 819. (c) Scaiano, J. C.; Lee, C.; Chow, Y.; Marciniak, B. *J. Phys. Chem.* **1982**, *86*, 2452.

(7) Closs, G. L.; Miller, R. J. *J. Am. Chem. Soc.* **1981**, *103*, 3586.

(8) (a) Lister, D.; MacDonald, J.; Owen, N. "Internal Rotation in Molecules"; Academic Press: New York, 1978. (b) Abe, A.; Jernigan, R.; Flory, P. J. *Am. Chem. Soc.* **1966**, *88*, 631.

(9) Doubleday, C.; Camp, R. N.; King, H. F.; McIver, J. W., Jr.; Mullally, D.; Page, M. *J. Am. Chem. Soc.* **1984**, *106*, 447.

(10) (a) Engel, P. S.; Keys, D. E. *J. Am. Chem. Soc.* **1982**, *104*, 6860. (b) Engel, P. S.; Horsey, D.; Keys, D.; Nalepha, C.; Soltero, L. *J. Am. Chem. Soc.* **1983**, *105*, 7108. (c) Engel, P.; Keys, D.; Kitamura, A. *J. Am. Chem. Soc.* **1985**, *107*, 4964.

(11) (a) Bernardi et al. (ref 11b) have located stationary points corresponding to **1a** and **1b** on the singlet PES which they claim to be minima. However full force constants were not calculated. In any case, they estimate that the barriers to product formation are less than 1 kcal. This makes them kinetically insignificant compared to the much larger entropic barrier of at least 4 kcal at 700 K reported in ref 9. Thus the essential feature of the singlet PES is that in spite of ripples on the surface the dynamics are controlled by entropy. (b) Bernardi, F.; Bottoni, A.; Tonachini, G.; Robb, M. A.; Schlegel, H. B. *Chem. Phys. Lett.* **1984**, *108*, 599. (c) Bernardi, F.; Bottoni, A.; Robb, M.; Schlegel, H. B.; Tonachini, B. *J. Am. Chem. Soc.* **1985**, *107*, 2260.

(12) For a recent example applied to triplet trimethylene, see: Yamaguchi, Y.; Schaefer, H. F., III *J. Am. Chem. Soc.* **1984**, *106*, 5115.

(13) (a) Glasstone, S.; Laidler, K.; Eyring, H. "Theory of Rate Processes"; McGraw-Hill: New York, 1941. (b) Robinson, P.; Holbrook, K. "Unimolecular Reactions"; Wiley-Interscience: New York, 1972.

(14) (a) Binkley, J.; Pople, J.; Hehre, W. *J. Am. Chem. Soc.* **1980**, *102*, 939. (b) Hariharan, P. C.; Pople, J. A. *Theor. Chim. Acta* **1973**, *28*, 213.

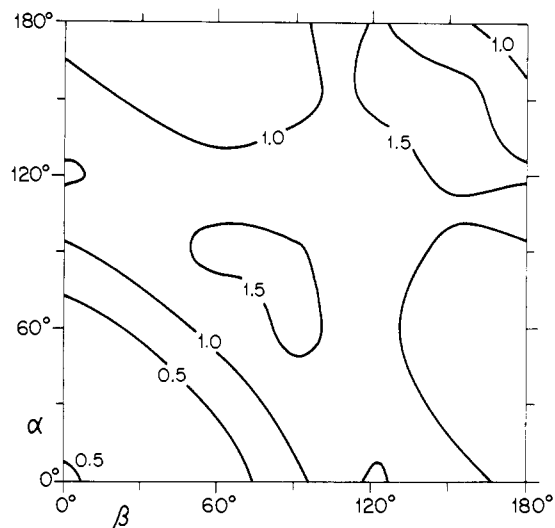


**Figure 2.** Singlet PES projected onto  $\alpha, \beta$ , with  $\gamma = 60^\circ$  and planar terminal methylenes. Contours of equal potential energy are in kcal/mol above the lowest grid point at (30,30,60).

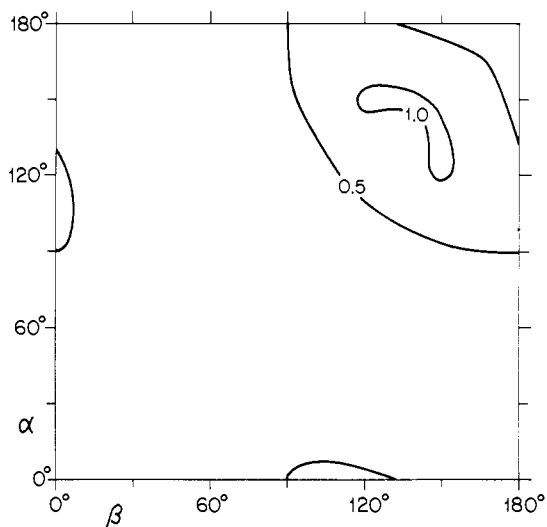


**Figure 3.** Triplet ( $\alpha, \beta, 60$ ) PES. Contours are in kcal/mol above the lowest grid point at (60,90,60).

simple case to 2-electron-2-orbital CASSCF.<sup>16</sup> For the triplet we also used a 2-electron, 2-orbital CASSCF which in this case is equivalent to the single configuration triplet. As we have discussed elsewhere,<sup>15</sup> 2CSCF with a split-valence basis set constitutes the minimum level of theory required for biradicals and appears to be good enough for semiquantitative reliability.

The coordinates are shown in Figure 1. A 3-dimensional  $\alpha, \beta, \gamma$  grid was calculated in the following way. With no pyramidalization of the terminal methylenes (planar arrangement,  $sp^2$  hybridization) we let  $\gamma$  take on the values of  $0, 60, 120, 180^\circ$ , and for each value of  $\gamma$  we varied  $\alpha$  and  $\beta$  independently from  $0^\circ$  to  $180^\circ$  in  $30^\circ$  increments. The (0,0,0) reference for each ( $\alpha, \beta, \gamma$ ) grid point is the  $C_{2v}$  geometry in Figure 1. At each grid point we calculated the energies of the singlet ( $E_S$ ) and triplet ( $E_T$ ), to obtain their difference  $E_{ST} = E_S - E_T$ .

### Results

Figures 2 and 3 show respectively  $E_S$  and  $E_T$  contours for  $\gamma = 60^\circ$  (1a). Figures 4–7 show the  $E_{ST}$  contour maps for all four values of  $\gamma$ . The shaded areas denote  $E_{ST} > 0$  (triplet ground

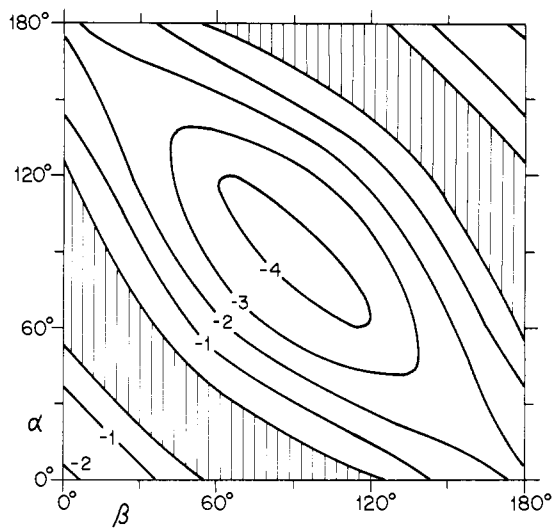


**Figure 4.**  $E_{ST}$  contours in kcal/mol as a function of  $\alpha$  and  $\beta$  with  $\gamma = 0^\circ$  and planar terminal methylenes. Shaded areas denote  $E_{ST} > 0$ .

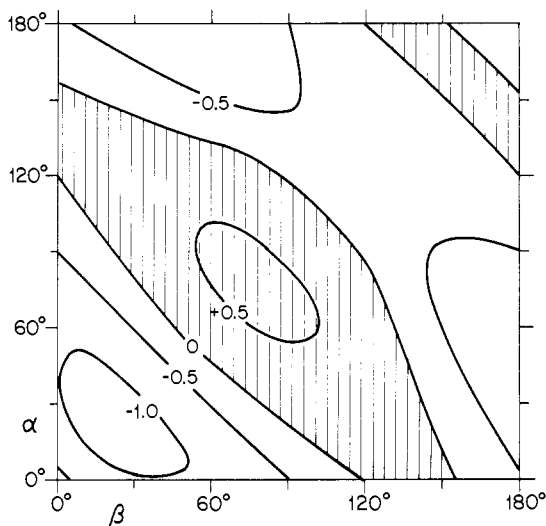


**Figure 5.**  $E_{ST}$  contours for  $\gamma = 60^\circ$ .

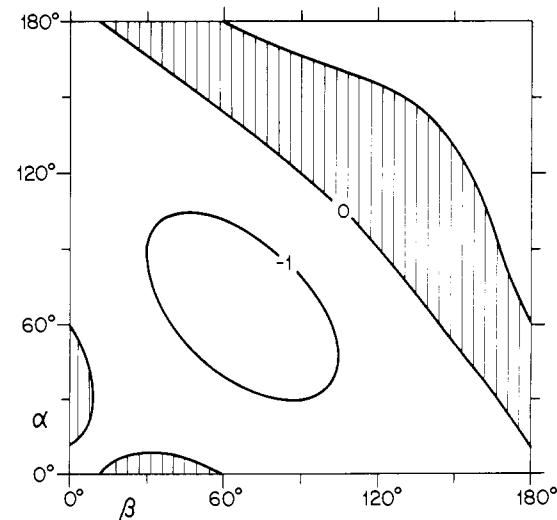


**Figure 6.**  $E_{ST}$  contours for  $\gamma = 120^\circ$ .

state). Except for  $\gamma = 0^\circ$ , both the singlet and triplet PES are relatively flat as a function of  $\alpha$  and  $\beta$ . This is shown in Figure 8, which plots the spread in  $E_S$  and  $E_T$  (minimum to maximum energy over the full range of  $\alpha, \beta$ ) for each value of  $\gamma$ . Also included in Figure 8 is the spread in  $E_S$  and  $E_T$  for  $\gamma = 60^\circ$  (1a)

(15) Doubleday, C.; McIver, J. W., Jr.; Page, M. *J. Am. Chem. Soc.* **1982**, *104*, 6533.

(16) (a) Camp, R. N.; King, H. F. *J. Chem. Phys.* **1982**, *77*, 3056. (b) Siegbahn, P.; Almlof, J.; Hieberg, A.; Roos, B.; Levy, B. *Phys. Scr.* **1980**, *21*, 323. (c) Roos, B.; Taylor, P.; Siegbahn, P. *Chem. Phys.* **1980**, *48*, 157.

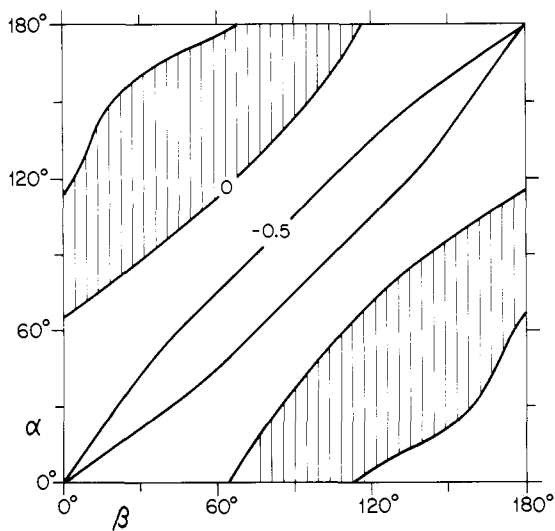


Figure 7.  $E_{ST}$  contours for  $\gamma = 180^\circ$ .

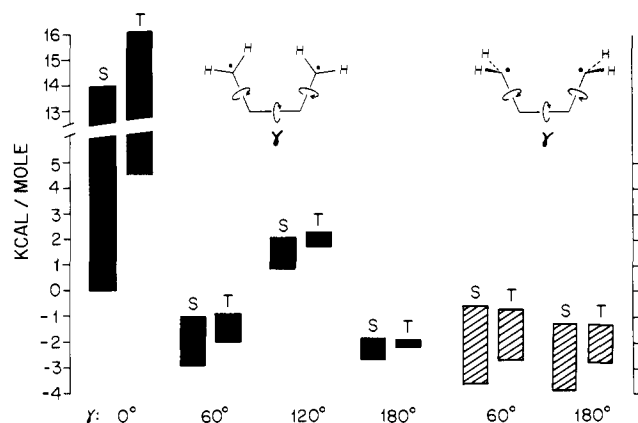


Figure 8. Spread in  $E_S$  and  $E_T$  (see text) for  $\gamma = 0^\circ, 60^\circ, 120^\circ, 180^\circ$  with planar terminal methylenes (first 4 pairs of bars) and for  $\gamma = 60^\circ, 180^\circ$  with pyramidalized methylenes (last two pairs of bars).

and  $\gamma = 180^\circ$  (**1b**) with the terminal methylenes pyramidalized  $16^\circ$  from planarity.<sup>18</sup> The  $E_{ST}$  contour plots for the pyramidal case are not shown because of their qualitative similarity to the plots with planar terminal methylenes. Figure 8 shows that all the  $\alpha, \beta$  surfaces are fairly flat except for  $\gamma = 0^\circ$ , where direct overlap between the ends is appreciable. Even here, although the total variation in  $E_S$  and  $E_T$  is 14.0 and 14.5 kcal, respectively, the two states are never more than 4.5 kcal apart. As  $\gamma$  increases to  $180^\circ$  the  $\alpha, \beta$  surfaces become flatter. This trend is less pronounced for pyramidal terminal methylenes. Although pyramidalization does increase the total variation in  $E_S$  and  $E_T$ , it has a small effect on the variations in  $E_{ST}$ . For  $\gamma = 60^\circ$ ,  $E_{ST}$  ranges from  $-1.1$  to  $+0.7$  kcal with planar methylenes and from  $-1.2$  to  $+0.5$  kcal with pyramidal methylenes. For  $\gamma = 180^\circ$ ,  $E_{ST}$  ranges from  $-0.7$  to  $+0.3$  kcal (planar) and from  $-1.4$  to  $+0.2$  kcal (pyramidal).

Finally, we examined two methyl radicals whose intercarbon distance, mutual angular orientation, and internal geometry exactly match the terminal methylenes of tetramethylene (planar terminal methylenes) and calculated all the  $E_S$  and  $E_T$  grid points analogous to Figures 4–7. This mimics a tetramethylene in which the only end-to-end interaction is through space. We have included two of the resulting  $E_{ST}$  contour plots, for  $\gamma = 0^\circ$  (Figure 9) and  $\gamma = 60^\circ$  (Figure 10).

(17) Bobrowicz, F.; Goddard, W. A., III "Methods of Electronic Structure Theory"; Schaefer, H. F., III, Ed.; Plenum Press: New York, 1977; pp 77–127.

(18) The pyramidalization angle of  $16^\circ$  is defined as the acute angle of intersection between the terminal C–C bond and the  $\text{CH}_2$  plane.

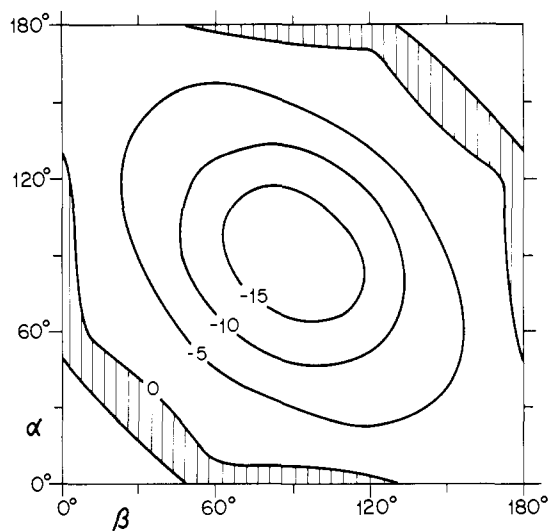


Figure 9.  $E_{ST}$  contours in kcal/mol for the methyl radical pair (see text) with mutual orientation identical with that of **1** with  $\gamma = 0^\circ$ .

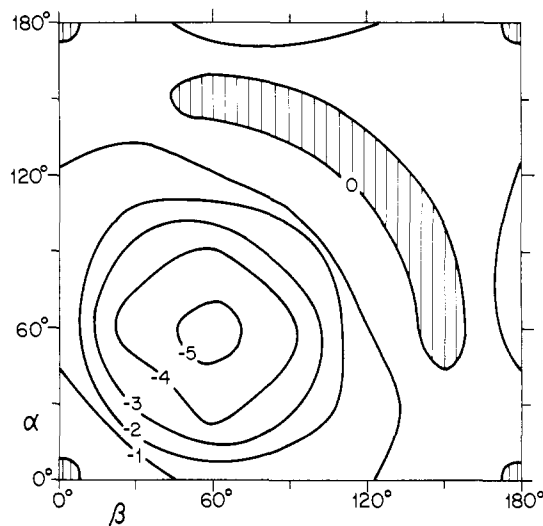


Figure 10.  $E_{ST}$  contours for the methyl radical pair with mutual orientation identical with that of **1** with  $\gamma = 60^\circ$ .

## Discussion

The level of theory applied here, 2CSCF with the 3-21G basis set, is not definitive. Certain details are probably not well described at this level, such as the exact location of stationary points and S–T intersections and the precise values of  $E_{ST}$  at a given geometry. Fortunately, these local features turn out not to be critical (see below). Qualitative, global features such as the large number of S–T intersections are, we feel, reasonably well predicted and should survive at any level of theory. In trimethylene, for example, changing the basis set from 3-21G<sup>14a</sup> to 6-31G\*<sup>14b</sup> has a minor effect on  $E_{ST}$ .<sup>15</sup> Also for trimethylene, Kato and Morokuma<sup>23</sup> found that adding configurations beyond the 2CSCF level has an extremely small effect on the singlet wave function. We expect

(19) An extensive discussion of the chemical effects of interaction via the  $\sigma$  bond framework is given in the following references. (a) Dewar, M. J. S. *Bull. Soc. Chim. Belg.* **1979**, *88*, 957. (b) Dewar, M. J. S.; McKee, M. L. *Pure Appl. Chem.* **1980**, *52*, 1431. (c) Verhoeven, J. W. *Recl. Trav. Chim. Pays-Bas* **1980**, *99*, 143. (d) Verhoeven, J. W. *Recl. Trav. Chim. Pays-Bas* **1980**, *99*, 369. (e) Verhoeven, J. W. *Tetrahedron* **1981**, *37*, 943.

(20) Goldberg, A. H.; Dougherty, D. A. *J. Am. Chem. Soc.* **1983**, *105*, 284.

(21) Grant, A.; Gren, N.; Hore, P.; McLauchlan, K. *Chem. Phys. Lett.* **1984**, *110*, 280.

(22) Kaptein, R.; vanLeeuwen, P.; Huis, R. *Chem. Phys. Lett.* **1976**, *41*, 264.

(23) Kato, S.; Morokuma, K. *Chem. Phys. Lett.* **1979**, *65*, 19.

the same to be true of tetramethylene.

The most significant feature of our results is that **1** corresponds to a broad, flat region of the singlet and triplet PES characterized by a *profusion of S-T intersections* encountered as a result of internal rotations. This finding is in qualitative agreement with the experimental results obtained by one of us<sup>3</sup> from a variety of 1,5- and 1,6-biradicals by means of the magnetic field dependence of <sup>13</sup>C CIDNP. These studies showed that internal rotation about C-C bonds in the biradicals is sufficient to produce S-T intersections.

Our calculations give a clear answer to the question of how well  $E_{ST}$  is predicted by a radical pair model in which the only end-to-end interaction is through space. Figures 9 and 10 show  $E_{ST}$  for a pair of methyl radicals with a mutual orientation identical with that of the terminal methylenes in **1**. For  $\gamma = 60^\circ$  (Figure 10), the radical pair model is inadequate. Comparison of the shaded regions (triplet ground state) of Figures 5 and 10 shows no commonality. An analogous qualitative dissimilarity between two methyls and **1** exists for  $\gamma = 120, 180^\circ$  (not shown). Only for  $\gamma = 0^\circ$  (Figures 4 and 9) is the radical pair model qualitatively acceptable. This is reasonable, since with incipient bond formation on the singlet surface one expects the direct interaction through space to be prominent.

Through-bond interaction certainly has a significant, even dominant, effect on  $E_{ST}$  over most of the PES.<sup>19</sup> We<sup>15</sup> and Dougherty<sup>20</sup> have found similar effects on  $E_{ST}$  in trimethylene. For 1,5-biradicals or larger, one expects through-bond interaction to decrease as the chain length increases.

A model for  $E_{ST}$  in biradicals advocated by deKanter and Kaptein<sup>4</sup> assumes that

$$E_{ST} = E_0 \exp(-ZR) \quad (1)$$

where  $E_0$  and  $Z$  are adjustable parameters and  $R$  is the end-to-end distance. Their model is not suitable for the purposes of this study because it does not allow  $E_{ST}$  to change sign, a prerequisite for isc. Equation 1 is also contradicted by CIDNP data.<sup>3b-d</sup> McLauchlan and co-workers,<sup>21</sup> following a suggestion of Kaptein,<sup>22</sup> have proposed

$$E_{ST} = E_1 \exp(-Z_1R) - E_2 \exp(-Z_2R) \quad (2)$$

for radical pairs on the basis of CIDEP results. The parameters are such that  $E_{ST} < 0$  for small  $R$  and  $E_{ST} > 0$  for large  $R$ .

Although  $E_{ST}$  is a complicated function of geometry, in certain symmetric cases it is easy to understand the effect of through-bond coupling on  $E_{ST}$ . For example, consider a  $\gamma$ -rotation beginning with (90,90,0) (p orbitals directed toward each other), followed by (90,90,60), (90,90,120), and (90,90,180). The common symmetry element is a  $C_2$  axis bisecting the central C-C bond. The top of Figure 11 explicitly considers a through-bond interaction in (90,90,180). By an argument originally given by Hoffmann,<sup>23</sup> the interaction of the symmetric (S) singly occupied MO with the bonding C-C  $\sigma$  MO pushes the singly occupied S MO up in energy. The antisymmetric (A) singly occupied MO is pushed down in energy by interaction with the antibonding  $\sigma$  MO. Thus through-bond interaction favors A below S, whereas through-space interaction favors S below A. The through-bond interaction is significant throughout the rotation, but through-space interaction drops off sharply as the overlap integral between the p-type AOs on the radical centers decreases. The middle portion of Figure 11 shows that this competition produces an S/A crossing during the rotation. At  $\gamma = 0^\circ$  the through-space interaction is dominant, and through-bond interaction takes over at  $\gamma = 120^\circ, 180^\circ$ . On the other hand, two methyl groups can only interact through space. Consequently S is always below A and they are virtually degenerate once  $\gamma$  reaches  $120^\circ$ .

The effect of orbital energies on  $E_{ST}$  can be predicted qualitatively by eq 3, which we derived previously and applied to trimethylene:<sup>15</sup>

$$E_{ST} = 2K_{14} + K_{SA} - [(\epsilon_S - \epsilon_A)^2 + K_{SA}^2]^{1/2} \quad (3)$$

Here  $K_{14}$  is the exchange integral over the p orbitals on  $C_1$  and  $C_4$ ,  $K_{SA}$  is the exchange integral over the MOs made from S and

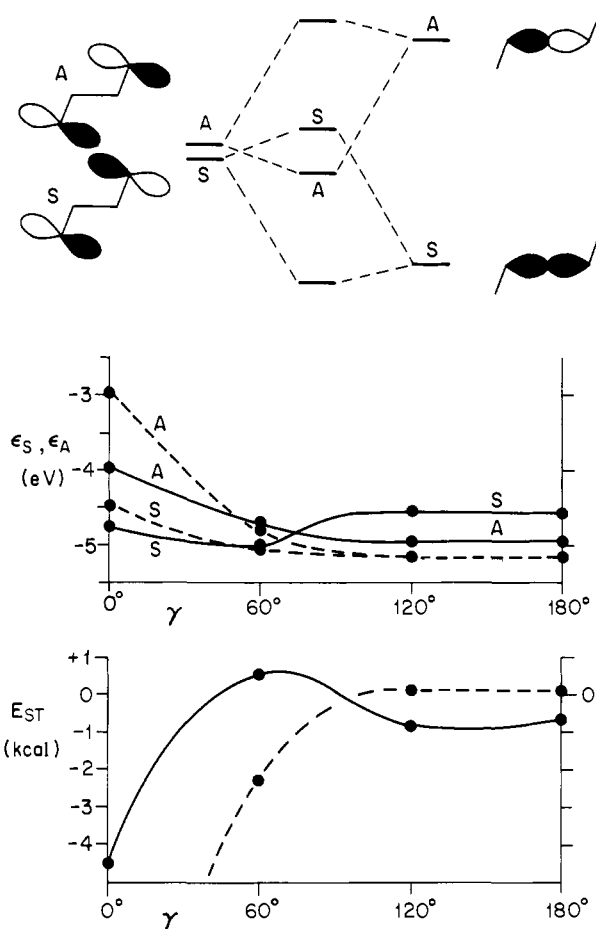


**Figure 11.** Effect of through-bond interaction in (90,90, $\gamma$ ) **1**. Top: interaction in (90,90,180) **1** between the singly occupied MOs and  $\sigma$  C-C MOs. Middle: orbital energies  $\epsilon_S$  and  $\epsilon_A$  as a function of  $\gamma$  for **1** (solid lines) and for the methyl radical apir (dashed lines). Bottom:  $E_{ST}$  as a function of  $\gamma$  for **1** (solid line) and the methyl pair (dashed line).

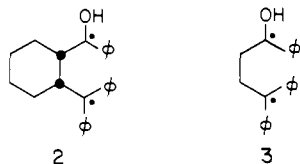
A combinations of these AOs (with respectively antibonding and bonding admixtures of the C-C  $\sigma$  MO), and  $\epsilon_S$  and  $\epsilon_A$  are the orbital energies of the S and A MOs. Since the exchange integrals are positive, eq 3 predicts a triplet ground state whenever  $|\epsilon_S - \epsilon_A|$  is smaller than some critical value. The bottom of Figure 11 shows that  $E_{ST} > 0$  only in the vicinity of the S/A crossing, where  $|\epsilon_S - \epsilon_A|$  is small. This accounts for the qualitative difference between the  $\gamma$  dependence of  $E_{ST}$  in **1** and in two methyl groups. Through-bond interaction also accounts for the large quantitative differences in  $E_{ST}$  of **1** vs. two methyls near (90,90,0), where through-space interaction is a maximum. From the middle of Figure 11 one sees that the large orbital energy difference of 1.5 eV in the methyl pair is reduced to 0.75 eV in **1** because through-bond interaction favors A below S. This 17.3-kcal difference in  $\epsilon_S - \epsilon_A$  becomes a 13.8-kcal difference in  $E_{ST}$  ( $E_{ST} = -4.5$  kcal for **1** and  $-18.3$  kcal for the methyl pair).

It is tempting to extend this analysis by partitioning  $E_{ST}$  for an arbitrary structure into through-space and through-bond contributions. As we have pointed out,<sup>15</sup> however, a clean separation into through-space and through-bond terms is possible only in certain symmetric cases, e.g., (90,90, $\gamma$ ) **1** or the (0,0) "edge-to-edge" trimethylene structure,<sup>15,20</sup> for which the coupling between the two terms is zero. For unsymmetrical biradical structures, essentially the entire PES, an exact separation of  $E_{ST}$  into through-space and through-bond contributions is not possible.

Since isc in tetramethylene occurs only at the S-T intersections, it is significant that S-T degeneracy is very easy to achieve in tetramethylene. In the 3-dimensional  $\alpha, \beta, \gamma$  grid of Figures 4-7, if two angles are fixed at virtually any arbitrary values and the third varied over  $180^\circ$ , two S-T intersections are encountered. The flatness of the triplet PES for **31a** (Figure 3) and **31b**

guarantees that all intersections are thermally accessible at room temperature or above.

If structural flexibility is sufficient for easy access to S-T intersections, is it also necessary? Recent work of Caldwell<sup>24</sup> shows that **2**, with  $\gamma$  fixed at ca. 60° and  $\alpha$  and  $\beta$  hindered, has an isc rate constant of  $1.45 \times 10^7 \text{ s}^{-1}$  at 25 °C in heptane, compared to the flexible analog **3**, with an isc rate constant of  $1.19 \times 10^7 \text{ s}^{-1}$  in heptane.<sup>24</sup> Thus partial removal of flexibility does not prevent access to S-T intersections needed for efficient isc.



Another important question is the structural dependence of the spin orbit coupling (SOC) matrix element. SOC in biradicals is strongly dependent on the relative angular orientation of the termini and decreases approximately exponentially with increasing end-to-end distance.<sup>25</sup> Recent experiments on 1,7- to 1,15-biradicals containing an acyl terminus have shown that SOC is the dominant isc mechanism<sup>26</sup> and that isc occurs mainly in geometries with small end-to-end distances.<sup>26c</sup> An accurate knowledge of SOC

is obviously required to understand isc in biradicals. Preliminary SOC calculations on trimethylene (based on the Breit-Pauli spin-orbit interaction<sup>27</sup>) have already appeared from this laboratory.<sup>28</sup> Further SOC calculations are in progress.<sup>29</sup>

In conclusion, 2-configuration MCSCF 3-21G calculations of the S-T energy gap  $E_{ST}$  were performed as a function of the three internal rotations and the pyramidalization of the terminal methylenes. Through-bond coupling is found to dominate the structural dependence of  $E_{ST}$ . We<sup>15</sup> and Dougherty<sup>20</sup> have found the same effect in trimethylene. The importance of through-bond coupling in larger biradicals is unknown since the effect is expected to attenuate with increasing chain length. For the isc process, our most important result is that at room temperature or above, a thermally equilibrated triplet tetramethylene cannot avoid encountering S-T intersections. However, the calculations are not sufficient to predict the product distribution. This contrasts with triplet trimethylene, for which we showed<sup>15</sup> that knowledge of the S and T surfaces are sufficient by themselves to correctly predict nearly exclusive cyclization. For triplet tetramethylene, a prediction of the product distribution as well as the isc rate constant would require a knowledge of SOC plus a dynamical treatment of the S-T crossing.

**Acknowledgment.** The authors thank Richard A. Caldwell, Gerhard L. Closs, and J. C. Scaiano for communicating their results prior to publication. We acknowledge the National Science Foundation for support.

(24) Caldwell, R. A.; Dawan, S.; Majima, T. *J. Am. Chem. Soc.* **1984**, *106*, 6454.

(25) Salem, L.; Rowland, C. *Angew. Chem., Int. Ed. Engl.* **1972**, *11*, 92.

(26) (a) Closs, G. L.; Redwine, O. D. *J. Am. Chem. Soc.* **1985**, *107*, 4543.

(b) Zimmt, M.; Doubleday, C.; Gould, I.; Turro, N. J. *J. Am. Chem. Soc.*, in press. (c) Zimmt, M.; Doubleday, C.; Turro, N. J. *J. Am. Chem. Soc.*, in press.

(27) Bethe, H.; Salpeter, E.; "Quantum Mechanics of One- and Two-Electron Atoms"; Springer: New York, 1957.

(28) Furlani, T.; King, H. *J. Chem. Phys.* **1985**, *82*, 5577.

(29) Carlacci, L.; Doubleday, C.; Furlani, T.; King, H.; McIver, J., to be published.

## Oxidation of 2,6-Di-*tert*-butylphenol by Molecular Oxygen. 2. Catalysis by Cobaltous Polyamine Chelates through Their ( $\mu$ -Peroxo)- and ( $\mu$ -Peroxo)( $\mu$ -hydroxo)dicobalt(III) Complexes

Stephen A. Bedell and Arthur E. Martell\*

Contribution from the Department of Chemistry, Texas A&M University, College Station, Texas 77843. Received January 14, 1985

**Abstract:** The oxidation of 2,6-di-*tert*-butylphenol by molecular oxygen is catalyzed by the cobaltous chelates of tetraethylenepentamine (TETREN), dipicolyl-diethylenetriamine (PYDIEN), and 1,4,10,13-tetraaza-7-thiatridecane (TATTD), through their ( $\mu$ -peroxo)dicobalt(III) complexes and by those of dipicolylethylenediamine (PYEN), tris(aminoethyl)amine (TREN), and triethylenetetramine (TRIE) through their ( $\mu$ -hydroxo)( $\mu$ -peroxo)dicobalt(III) complexes. Reaction products are identified as the oxidative coupling product 3,3',5,5'-tetra-*tert*-butyldiphenoquinone and the partial oxygen insertion product, 2,6-di-*tert*-butylbenzoquinone. The rates of reaction of the substrate as well as the formation of products are shown to be first order with respect to the concentrations of both the cobalt-dioxygen complex and the substrate. The reaction with  $[\text{Co}_2(\text{TETREN})_2\text{O}_2]^{4+}$  does not occur in the absence of free molecular oxygen in solution and occurs at a reduced rate under air relative to oxygen.

The role of cobalt-dioxygen complexes in the oxidation of organic substrates, most notably hindered phenols, is the objective of several recent reports.<sup>1-3</sup> Following pioneering work by Van Dort and Geurson<sup>4</sup> on the salcomine ([bis(salicylaldehyde)

ethyleneimine]cobalt(II))-catalyzed oxidation of 2,6-substituted phenols to produce substituted benzoquinones and diphenoquinones, Nishinaga carried out extensive studies on such systems,<sup>5,6</sup> demonstrating the role of the phenoxy radical, which is the first intermediate in the formation of the oxidized coupled product. A significant contribution to the cobalt Schiff-base-

(1) Nishinaga, A.; Tomita, H.; Nishizawa, K.; Matsuura, J. *J. Chem. Soc., Dalton Trans.* **1981**, 1504.

(2) Bedell, S. A.; Martell, A. E. *Inorg. Chem.* **1983**, *22*, 364.

(3) Wang, X. Y.; Motekaitis, R. J.; Martell, A. E. *Inorg. Chem.* **1984**, *23*, 271.

(4) Van Dort, H. M.; Geurson, H. J. *Recl. Trav. Chim. Pays-Bas.* **1967**, *86*, 520.

(5) Nishinaga, A. "Biochemical and Medical Aspects of Active Oxygen"; Hayaishi, O., Asada, K., Eds.; University Park Press: Baltimore, MD, 1977; p 13.

(6) Nishinaga, A.; Tomita, H.; Shimizu, T.; Matsuura, T. *Fundam. Res. Homogeneous Catal.* **1978**, *2*, 241.